

Confinement and zone folding in the E_1 -like optical transitions of Ge/Si quantum wells and superlattices

P. A. M. Rodrigues, M. A. Araújo Silva, and F. Cerdeira

Instituto de Física "Gleb Wataghin," Universidade Estadual de Campinas, Unicamp, 13083-970 Campinas, São Paulo, Brazil

J. C. Bean

AT&T Bell Laboratories, Murray Hill, New Jersey 07974

(Received 17 August 1993)

We report low-temperature (77 K) electroreflectance and photorefectance measurements of the E_1 -like optical transitions on a series of Ge/Si heterostructures (superlattices and quantum wells). For single and double quantum wells of any thickness, as well as for thick-layer superlattices (period ~ 100 Å) the spectra can be understood in terms of quantum-confined bulk-Ge E_1 states. For thin (~ 10 Å) multiple quantum wells and superlattices, zone-folding effects dominate the spectra. Actual confinement of the electronic states is determined by measuring the Raman spectrum of each sample in and out of resonance with a given transition.

INTRODUCTION

The study of the electronic states in pseudomorphically grown Ge/Si heterostructures poses many challenging questions, such as the possibility of producing a pseudo-direct-gap material through zone folding.^{1,2} The electronic band structure of Ge/Si superlattices has been calculated using several theoretical methods³⁻⁶ and probed by different experimental techniques.⁷⁻¹³

Earlier workers focused their interest in the structurally induced quasidirect gap in short-period superlattices and only recently has attention been drawn to the higher interband transitions.^{10,12,13}

We are interested here in structures in the optical spectrum of single and multilayered Ge/Si systems related to the bulk E_1 transitions. These are direct transitions between valence and conduction bands, which run parallel along the [111]-direction (Λ line) of the Brillouin zone, all the way to the zone edge (point L).¹⁴ When constructing the electronic states of Ge/Si multilayered systems using those of their bulk constituents, empirical concepts such as those of single (SQW) or multiple quantum wells (MQW) are used. The applicability of these concepts to electronic states derived from zone-center bulk states has been established, even for very thin Ge_nSi_m structures.^{15,13} The main consequences of the QW model on zone-center states are those of confining the bulk states to the Ge layers and the miniband formation in superlattices. For bulk states with $\mathbf{k} \neq \mathbf{0}$ in a periodic Ge_nSi_m structure zone folding should occur. Theoretical^{3,4} and experimental^{12,13} information on this type of superlattice indicates that the E_1 bulk transitions split into multiplets as a result of zone-folding and the consequent repulsion between zone-folded states. The concept of confinement is more difficult to apply to the states involved in these transitions. Although the E_1 gap is larger in bulk-Si (3.5 eV) (Ref. 16) than in

bulk-Ge (2.3 eV),¹⁴ the width of the individual conduction and valence band is considerable ($\Delta \sim 0.6$ eV), since the bands run through a large fraction ($\sim 70\%$) of the Γ - $L(\Lambda)$ line. In fact, both in III-V structures or in $\text{Ge}/\text{Ge}_x\text{Si}_{1-x}$ quantum wells and superlattices this spread is larger than the difference in the E_1 optical gap of the constituent materials. Under these conditions it is difficult to see why the electronic wave function should be confined within the smaller gap constituent. In spite of this, evidence of this type of confinement for E_1 -like structures has been reported in some superlattices based on III-V materials.^{17,18} Also, ellipsometric and resonant Raman scattering measurements in single Ge layers of thicknesses down to 7 Å show optical structures that can be unambiguously attributed to E_1 -like transitions confined in the Ge layers.^{11,19} As mentioned before, when, instead of a single Ge layer, we have a Ge_nSi_m periodic structure, the confined E_1 -like mode evolves into a multiplet. Results of resonant Raman scattering⁸ and modulated reflectivity¹³ suggest that this multiplet is composed of two distinct components: a Ge-like doublet and a Si-like one at lower and higher energies, respectively. It is not clear, however, how this transition from a single confined state to a multiplet of Ge-like and Si-like character takes places. It is also not clear whether the concept of confinement of E_1 -like states survives in shallower quantum wells, such as those in $\text{Ge}/\text{Ge}_x\text{Si}_{1-x}$ systems.

In an effort to clarify the issues discussed above, we have performed modulated reflectivity (MR) and resonant Raman scattering (RRS) measurements in several Ge/Si and $\text{Ge}/\text{Ge}_x\text{Si}_{1-x}$ heterostructures, which provide a series of quantum wells with varying depth, width, and number of repetitions. In the $\text{Ge}/\text{Ge}_x\text{Si}_{1-x}$ superlattices, the shallow quantum wells produce E_1 -like transitions clearly derived from bulk-Ge E_1 states. A similar result is observed in a single Ge layer [five monolayers (ML) thick] embedded in a Si matrix. In both cases the E_1 -

like structure is shifted toward higher energies from the bulk E_1 -peak and this shift increases as the width of the Ge layer decreases. This is consistent with the idea of quantum confinement. Actual confinement of the electronic wave function is confirmed by measuring the Raman spectrum at and off-resonance with this transition. For double and sextuple (5 ML) quantum wells of Ge in a Si matrix there is a continuous evolution toward the E_1 -multiplet reported in Ref. 13. The Ge-like character of the two lowest energy members of this multiplet is confirmed by resonant Raman scattering measurements.

EXPERIMENTAL DETAILS

The samples were grown by molecular beam epitaxy at low substrate temperatures.²⁰ Those with thick ($d \sim 100$ Å) Ge layers were grown on Ge(001) substrates and are composed of alternating layers of Ge and $\text{Ge}_x\text{Si}_{1-x}$ alloy. The samples with thin ($d \sim 5$ ML) Ge layers were grown on Si(001) substrates. There are three such samples consisting of a single (1QW), a double (2QW), and a sextuple (6QW) Ge quantum well. In multiple quantum well samples the Ge layers (~ 5 ML thick) are separated by 5 ML of pure Si, acting as a barrier material. Each of these structures (single, double, or sextuple wells) is repeated ten times, having 300-Å-thick Si spacer layers between them. Structural parameters were checked with x-ray diffraction¹⁵ and Raman scattering.^{21,22} All relevant sample parameters are listed in Table I.

The electroreflectance (ER) and photoreflectance (PR) measurements were performed at 77 K with the samples immersed in liquid nitrogen, using a standard setup.²³ For ER measurements a Schottky barrier was created by depositing a $\simeq 100$ -Å-thick Ni-film on the sample surface. The modulation was accomplished by biasing externally the Schottky barrier with an ac voltage of $\simeq 3$ V peak to peak. For PR measurements the secondary (modulation) beam comes from a 10 mW He-Cd laser attenuated by neutral filters and mechanically chopped at 200 Hz. The experimental spectra were fitted with a third derivative line shape:²³

TABLE I. Relevant structural parameters of the samples studied. The column d_A (d_B) lists the thickness of the Ge ($\text{Ge}_x\text{Si}_{1-x}$) layers, x is the Ge concentration in the alloy $\text{Ge}_x\text{Si}_{1-x}$, ϵ^{Ge} is the percentage variation of the in-plane lattice parameter of the heterostructure and that of bulk Ge, while N is the number of times the structure d_A/d_B was repeated.

Sample	d_A (Å)	d_B (Å)	x	$10^2 \epsilon^{\text{Ge}}$	N
SLA	102 ^a	34 ^a	0.7 ^a	$\sim 0^a$	15 ^b
SLB	111 ^a	32 ^a	0.7 ^a	$\sim 0^a$	20 ^b
1QW	7.3 ^b	0	0	-4.01 ^b	1 ^b
2QW	7.3 ^b	6.8 ^b	0	-4.01 ^b	2 ^b
6QW	7.3 ^b	6.8 ^b	0	-4.01 ^b	6 ^b

^aExperimental value. See Ref. 15.

^bNominal value.

$$\frac{\Delta R}{R} = \sum_j \text{Re} \left\{ \frac{C_j e^{i\theta_j}}{[(\hbar\omega - E_j) + i\Gamma_j]^n} \right\}, \quad (1)$$

where j is the transition number, C_j the relative amplitude, θ_j the phase, Γ_j the phenomenological broadening parameter, and E_j the transition energy. We used $n = 3.0$ which corresponds to two-dimensional critical points.

Raman scattering measurements were performed on all samples. These served both as a characterization of structural parameters such as strain²¹ and periodicity,²² and to obtain information as to the confinement of the electronic states in a given optical transition.^{24,8,19} Several lines of Ar-ion and Kr-ion lasers were used as exciting radiation. Scattered light was analyzed by a SPEX 1401 monochromator with standard photon-counting detection. All measurements were performed at room temperature in the backscattering configuration. Normalized Raman intensities were obtained by dividing the intensity of the Raman features of the Ge/Si samples by that of the Si optical phonon peak from a piece of bulk Si placed next to the samples.

RESULTS AND DISCUSSION

Modulated reflectivity

Figure 1 shows PR spectra of the two $\text{Ge}/\text{Ge}_x\text{Si}_{1-x}$ superlattices (SLA and SLB) and of bulk Ge in the photon energy region where E_1 , $E_1 + \Delta_1$ transitions occur

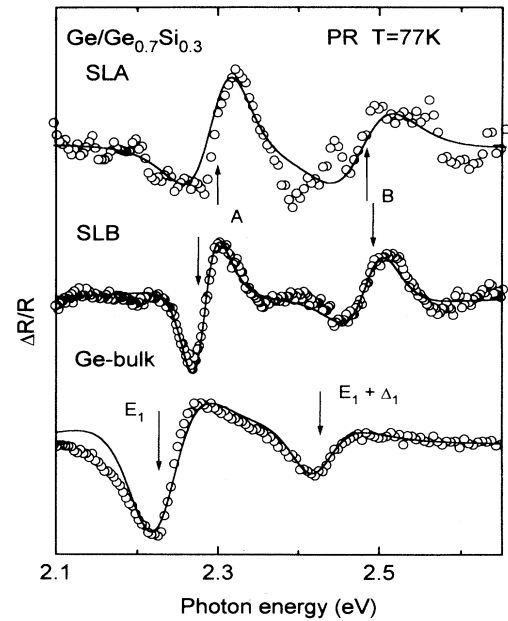


FIG. 1. Photoreflectance (samples SLA and SLB) and electroreflectance (Ge bulk) spectra in the range of the E_1 , $E_1 + \Delta_1$ transitions. Open circles are experimental data. The arrows are the transition energies obtained by the fitting procedure (continuous lines).

in the latter. All spectra show only two peaks in this region, the transition energies of which are obtained by fitting the experimental spectra (open circles) with the line shapes of Eq. (1) (solid lines). These transition energies are listed in Table II. The only difference between the spectral lines of the superlattices and that of bulk Ge, in this photon energy region, is that the lines in the former are slightly shifted toward higher energies. These shifts (72 meV for SLA and 52 meV for SLB) decrease as the thickness of the Ge layer increases. These facts lead to the identification of the spectral lines in Fig. 1 as originating in E_1 -transitions confined in the Ge layers of the $\text{Ge}/\text{Ge}_x\text{Si}_{1-x}$ superlattice. The actual confinement of the electronic states is verified by the resonant Raman results, which we shall discuss in the next subsection. A gross estimate of the confinement energy, obtained by calculating the ground state of a particle of mass μ (reduced interband mass from Ref. 25) in an infinite square well of appropriate thickness, predicts a 53 meV shift for SLA and a 45 meV shift for SLB. Given the naivety of the model, the good agreement of these numbers with our experimental results is probably fortuitous.

Let us turn to the thin layer heterostructures. In the inset of Fig. 2 we display the ER spectra of the 6QW, together with that of bulk Si. The spectra of the Ge quantum wells can be divided in three regions. In the spectral range $\hbar\omega \leq 2.4$ eV there is an oscillatory pattern produced by interferences due to the multiple reflections in the heterostructure/substrate interface. This pattern is also reported in ER (Ref. 13) and ellipsometric measurements¹² on strain-symmetrized Ge/Si superlattices. In contrast to a real modulated reflectance signal,

TABLE II. Transition energies (E_j), broadening parameter (Γ_j), and assignment for the E_1 -like transitions observed in the modulated reflectivity (MR) spectra of the Ge/Si heterostructures. The column "Confinement" lists the localization of the electronic wave functions corresponding to the E_1 -like transitions, obtained by resonant Raman scattering (RRS).

Sample	MR (77 K) $E_j(\Gamma_j)$ (in eV)	Assignment	Confinement RRS (300 K)
SLA	2.30 (0.07) A	E_1 (Ge)	Ge
	2.48 (0.09) B	$E_1 + \Delta_1$ (Ge)	
SLB	2.28 (0.04) A	E_1 (Ge)	Ge
	2.490 (0.06) B	$E_1 + \Delta_1$ (Ge)	
Ge-bulk (unstrained)	2.228 (0.08)	E_1	
	2.420 (0.07)	$E_1 + \Delta_1$	
$\text{Ge}_{0.7}\text{Si}_{0.3}$ -bulk ^a (strained)	2.524	E_1	
	2.728	$E_1 + \Delta_1$	
1QW	2.83 (0.11) A	E_1	Ge
2QW	2.72 (0.17) A	E_1^+	Mostly Ge
	2.98 (0.18) B	E_1^-	Mostly Si
6QW	2.43 (0.12) A	E_1^a	Mostly Ge
	2.59 (0.10) B	E_1^b	Mostly Ge
	2.74 (0.15) C	E_1^c	Mostly Si
	2.97 (0.12) D	E_1^d	Mostly Si

^aCalculated using the bulk unstrained alloy values and deformation potential theory (see Ref. 26).

the oscillations appearing in the spectra as a result of interference have an exponentially decaying amplitude for photon frequencies above the absorption edge of the superlattice. This damping, shown by dotted lines in the inset of Fig. 2, can be used to separate the modulation signal from interference artifacts as well as for estimating the absorption edge of the superlattice.^{12,13} For $\hbar\omega \simeq 3.2$ – 3.4 eV the spectra show an intense structure, easily identified with the $E_1-E'_0$ complex of bulk Si.¹⁶ Finally, in the region $\hbar\omega \sim 2.4$ – 3.1 eV the spectra contain peaks related to the Ge/Si heterostructures. We shall concentrate our discussion in this spectral region, for which Fig. 2 shows the best fit (continuous lines) to the experimental data (open circles) for all three samples. The individual line shapes composing the fit are shown below each spectra. The arrows, labeled by capital letters, indicate the transition energies obtained by the fitting procedure. The results from this fit and the assignment given to peaks A–D in Fig. 2 are listed in Table II.

The spectrum of the single quantum well (1QW) shows only one structure located at 2.83 eV (peak A in Fig. 2). Again, our resonant Raman scattering measurements (next subsection) show that this transition originates in electronic states confined within the 5 ML Ge quantum

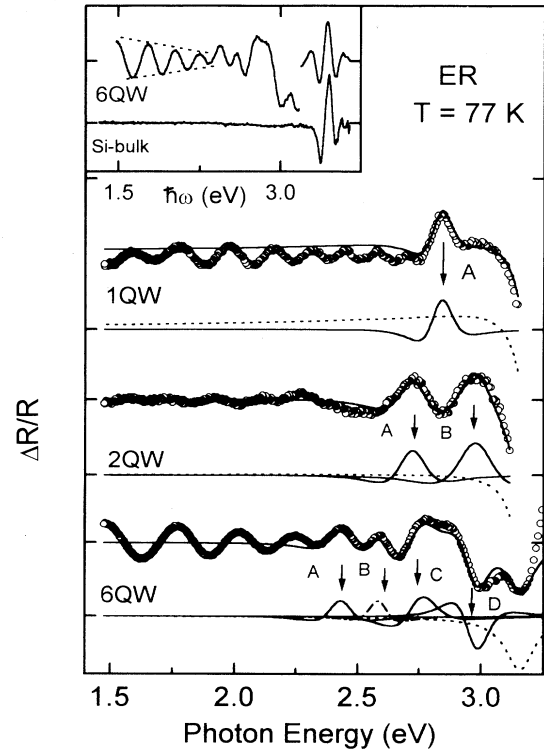


FIG. 2. Fittings (continuous lines) of the electroreflectance spectra for the samples 1QW, 2QW, and 6QW. The arrows indicate the transition energies obtained by the fitting procedure. The dotted lines are the functions fitted to the low energy side of the $E_1-E'_0$ bulk-Si complex. The inset shows the electroreflectance spectra of the sample 6QW and bulk Si. The dotted lines are meant as a guide to the interference pattern.

well. Given the thickness of the quantum well, this transition could either be E_0 -like or E_1 -like. However, the ER spectra of the Ge/Si superlattices show that the E_1 -like transitions are much stronger than the E_0 ones.¹³ Hence, we identify peak *A* with the E_1 -like transition of the Ge layer. This assignment is in consonance with the ellipsometric and resonant Raman scattering results of Ref. 11. Peak *A* in the spectrum of the 1QW is shifted to higher energies (490 meV) in comparison with the corresponding transition in the strained²⁶ bulk Ge. Although this shift can be attributed to quantum confinement, an infinite quantum well calculation of the confinement energy greatly overestimates this shift. The spectrum of the 2QW shows two structures (labeled *A* and *B* in Fig. 2) with almost the same intensities. Based on similar arguments as those for the sample 1QW, we assign the peaks *A* and *B* to E_1 -like transitions of the 2QW. The most striking change in the ER spectra when we go from the 1QW to the 2QW is the splitting of the E_1 -like transitions. This splitting suggests that the two peaks in the 2QW spectrum may be associated with transitions between symmetric and antisymmetric states in a double quantum well. Finally, the spectrum of the 6QW (lower curve in Fig. 2) is qualitatively different from those discussed above. The appearance of four structures suggests that the spectrum of the sextuple quantum well is similar to that of an infinite Ge_5Si_5 superlattice. The calculated band structure for an infinite strain-symmetrized Ge_5Si_5 superlattice⁴ predicts the existence of four E_1 -like critical points. The ER spectra for a Ge_5Si_5 sample with ~ 150 repetitions are compatible with this prediction.¹³ Differences in the strain profile are expected to change slightly the transition energy of each critical point, but not the number and character of the critical points. Therefore, we assign the structures *A*, *B*, *C*, and *D* present in the

spectrum of sample 6QW to the E_1^a , E_1^b , E_1^c , and E_1^d transitions predicted by the theoretical calculation for an infinite superlattice⁴ and reported in the ER spectra of Ref. 13.

The evolution of the E_1 -like region of the spectrum from one peak in a single quantum well to a multiplet in a Ge_nSi_m superlattice is illustrated in Fig. 3. Here we show the experimental energy of the E_1 -like transitions for the samples 1QW, 2QW, and 6QW as a function of the number of Ge layers (N). This figure also shows the corresponding transition energies for a strain-symmetrized Ge_5Si_5 superlattice, taken from Ref. 13. The arrows on the right side indicate the position of the relevant electronic transitions in bulk Ge (compressed) and bulk Si (not strained). Notice the reasonable agreement between the transition energies for the E_1 -like structures in the sample 6QW and a Ge_5Si_5 superlattice with 150 periods. This agreement is particularly good if we consider that the two samples have different strain profiles.

Raman scattering

Raman scattering can be used as a tool for structural characterization, giving information about strain, layer thickness, and periodicity.^{22,27–29} The Raman spectra of Ge_nSi_m superlattices exhibit three main peaks originating in optical vibrations. These are known as the Ge-Ge ($\sim 310 \text{ cm}^{-1}$), the Ge-Si ($\sim 415 \text{ cm}^{-1}$), and the Si-Si ($\sim 510 \text{ cm}^{-1}$) peaks.^{22,28–30} The Ge-Ge and Si-Si vibrations are confined in the Ge and Si layers, respectively. For the Ge-Ge mode this would seem surprising, since their frequency overlaps with the upper part of the Si acoustical branch and, therefore, this vibration could also propagate in the Si layer. However, such tunneling is known to be small and the vibrations remain practically confined within the Ge layers even in extreme cases such as $n \simeq m \simeq 4$ and $n \simeq 5$, $m \rightarrow \infty$. Their frequency can be obtained from the bulk modes, once strain and confining effects are taken into account. The Ge-Si modes are produced by vibrations at the interface, and have maximum amplitude there.^{22,28–30} These superlattice modes are not to be confused with the three modes (Ge-Ge, Ge-Si, and Si-Si) appearing in the spectra of $\text{Ge}_x\text{Si}_{1-x}$ alloys in similar frequency ranges.³¹ In fact, comparison between the true superlattice modes and those of the bulk alloys gives useful information about the abruptness of the interfaces in the former.²² In a $\text{Ge}/\text{Ge}_x\text{Si}_{1-x}$ superlattice there are two types of Ge-Ge modes: bulk Ge-like modes, localized in the Ge layers, and Ge-Ge alloy modes confined in the alloy layers. The remaining two alloylike modes (Ge-Si and Si-Si) also appear in the spectrum and they are expected to be localized in the alloy layers.

Figure 4 shows the Raman spectra of our samples and that of a thick (unstrained) $\text{Ge}_{0.5}\text{Si}_{0.5}$ alloy deposited on a Si(001) substrate. A sharp peak at 520 cm^{-1} appears in all our samples grown on Si substrates and corresponds to the bulk Si Raman line originating in the substrate, buffer layer, and spacer layers (in the nQW's samples). The spectra chosen for display in this figure were

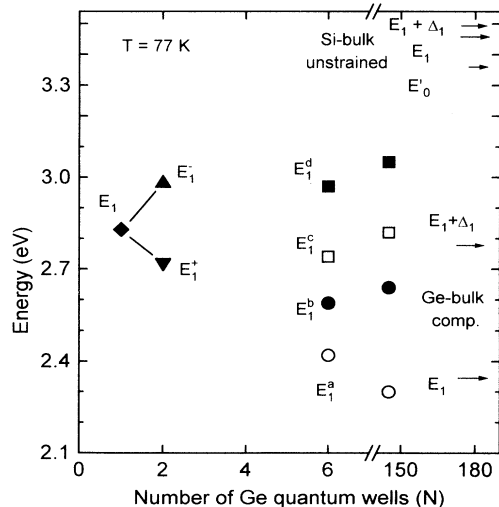


FIG. 3. Dependence of the E_1 -like transition energies with the number of the Ge quantum wells (N). The data for $N = 145$ were taken from Ref. 13. Notice the break in the horizontal scale. The arrows at the right side indicate the position of the relevant electronic transitions in bulk-Ge (compressed) and bulk-Si (not strained).

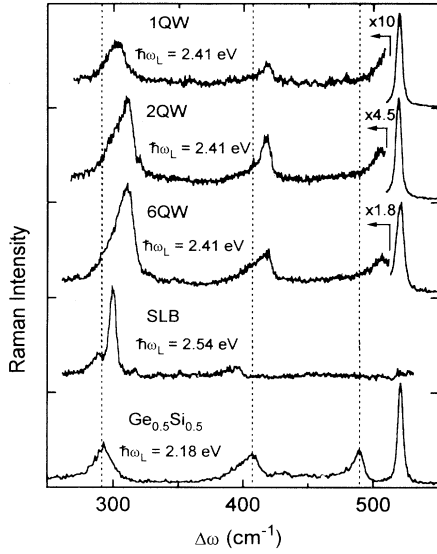


FIG. 4. Room temperature Raman spectra of our samples. The laser excitation energy ($\hbar\omega_L$) used to produce each spectrum is shown.

those taken with a laser excitation line which enhanced the weakest features in each spectrum, so that all spectral features from each sample are shown. Vertical lines through the alloy peaks are meant to facilitate the distinction between features arising from alloying and those produced by the quantum well structures. The clear differentiation between these features shows the good quality of the interfaces in our samples. We call attention to two particular spectral features. In the 2QW and 6QW samples a peak appears just below the bulk-Si peak. The facts that (i) this peak occurs at a higher frequency than that of the Si-Si peak of the alloy, and (ii) it is absent in the 1QW sample, allow us to identify this peak unambiguously as the Si-Si vibration of the 5-ML Si barrier, downshifted in energy from its bulk counterpart by confinement. The other feature is the pair of Ge-Ge peaks exhibited by the Ge/Ge_{0.7}Si_{0.3} superlattice (SLB). The one at lower frequency ($\omega_x \simeq 292 \text{ cm}^{-1}$) is clearly an alloy mode while the higher frequency member of this pair ($\omega_{SL} \simeq 300 \text{ cm}^{-1}$) is the Ge-Ge mode of the Ge layers of sample SLB. This identification is even clearer when the exciting laser frequency is changed. As we shall see next, when $\hbar\omega_L \simeq 2.2 \text{ eV}$ (in approximate resonance with the Ge E_1 -transition) this is the only line observable in the spectrum of the SLB sample (inset of Fig. 5).

Next we discuss the relative intensities of these Raman lines as a function of the exciting laser frequency ($\hbar\omega_L$). Resonant Raman scattering has been widely used, not only to determine electronic transition energies in quantum wells and superlattices, but also to obtain information about wave function confinement in these systems.^{8,11,18,19,24} This is accomplished by noticing that the Raman cross section of a given vibration will only be enhanced when $\hbar\omega_L$ (or $\hbar\omega_S$) is close to an electronic transition localized in the same layer as the vibration.

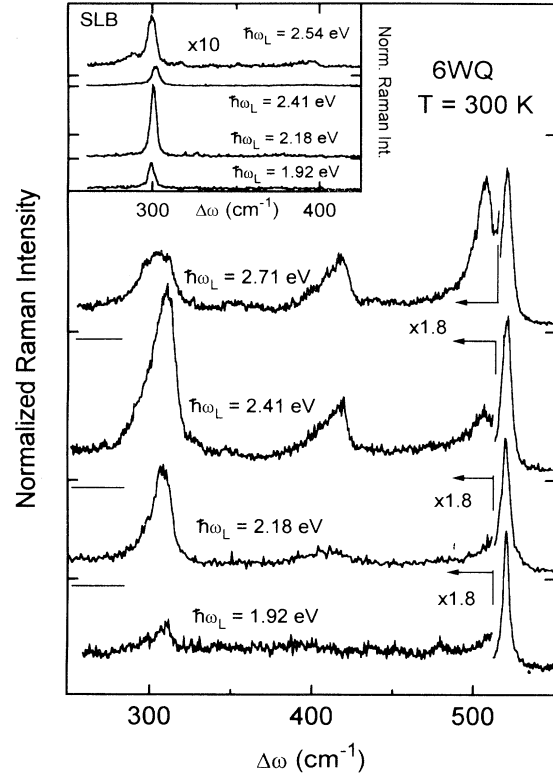


FIG. 5. Raman spectra of the sextuple quantum well (6QW) sample for different laser excitation energies ($\hbar\omega_L$). The intensity has been normalized to that of bulk Si (see text). The inset shows similar results for one of the Ge/Ge_{0.7}Si_{0.3} superlattices.

Thus, in order to determine whether a given electronic transition appearing in the modulated reflectivity (MR) spectrum is localized, we studied the Raman spectrum of the sample with $\hbar\omega_L$ in and off resonance with this transition. Representative results of this procedure are shown in Fig. 5, where the normalized Raman spectra of the 6QW sample is shown for various laser frequencies (the same is done for the SLB sample in the inset). In the SLB sample (inset of Fig. 5) the Ge peak shows a strong resonance at $\hbar\omega_L \simeq 2.18 \text{ eV}$, which is very close to the room temperature value of the E_1 -like transition observed in the ER spectrum.³² At this exciting frequency the spectral features from the alloy layers are not visible. They become apparent only when the laser frequency is in resonance with the E_1 transition of the strained Ge_{0.7}Si_{0.3} layer ($\hbar\omega_L = 2.54 \text{ eV}$, as seen in the inset of Fig. 5). This shows conclusively that the E_1 -like transition in the superlattice observed in the MR spectrum (Table II) is confined in the Ge layers.

Figure 5 shows that in the 6QW sample, the Ge peak has maximum intensity at $\hbar\omega_L = 2.41 \text{ eV}$, which coincides with the room temperature doublet E_1^a and E_1^b .³² For laser frequencies below this, the Si confined vibrations do not appear in the spectra of this sample. This peak increases in relative (and absolute) intensity as the laser frequency increases, reaching its highest value at

$\hbar\omega_L = 2.71$ eV (room temperature value of the E_1^c and E_1^d doublet; see Ref. 32). This indicates that the first (second) doublet originates in states mainly localized in the Ge (Si) layers. This localization is, however, not complete, since the Si peak is weakly enhanced when $\hbar\omega_L$ is in resonance with the first doublet. An entirely analogous situation arises in the 2QW sample (not shown in Fig. 5) where the E_1^+ (E_1^-) structure is shown to be mainly localized in the Ge (Si) layers. As for the 1QW (also not shown) resonant Raman scattering shows that the E_1 feature in the spectrum is localized in the Ge layers. This observation is in complete agreement with those of Refs. 11 and 19. The last column in Table II summarizes the conclusions about electronic wave-function localization obtained from our Raman measurements.

CONCLUSIONS

The results of the preceding section lead to the following picture in relation to the E_1 -like transitions of Ge/Si quantum wells and superlattices. In single Ge quantum wells confinement of the Λ -line electronic states occurs, as shown by the Raman results, leading to an increase in the transition energy. The evolution from a single to a double Ge layer still obeys the intuitive thinking

generated by the quantum well picture. In a Ge_nSi_m structure, with as few as six periods, the spectrum shows the full complexity of an infinite superlattice.^{12,13} In this case, zone-folding can be invoked and transitions separate clearly into pairs which have Ge-like and Si-like behavior. As the thickness of the superlattice increases, this separation is emphasized and the E_1^a and E_1^b can be thought of as the confined E_1 and $E_1 + \Delta_1$ transitions of bulk Ge. This suggests that, even in this complex case of electronic states spanning a considerable fraction of the Λ -line of the Brillouin zone and having a large energy spread, concepts such as zone-folding and confinement, derived from simple Krönig-Penney type models, apply. The generation of the appropriate periodic potential for quantitative predictions, however, is far from obvious to us at this point.

ACKNOWLEDGMENTS

This work was partially funded by the Third World Academy of Sciences, Fundação de Amparo à Pesquisa do Estado de São Paulo, and Conselho Nacional de Desenvolvimento Científico e Tecnológico (Brazil).

-
- ¹ T. P. Pearsall, CRC Crit. Rev. Solid State Mater. Sci. **15**, 551 (1989).
 - ² R. People and S. A. Jackson, in *Semiconductors and Semimetals*, edited by T. P. Pearsall (Academic Press, New York, 1991), Vol. 32, p. 119.
 - ³ M. S. Hybertsen and M. Schlüter, Phys. Rev. B **36**, 9683 (1987).
 - ⁴ U. Schmid, N. E. Christensen, M. Alouani, and M. Cardona, Phys. Rev. B **43**, 14 597 (1991), and references cited therein.
 - ⁵ S. Froyen, D. M. Wood, and A. Zunger, Phys. Rev. B **36**, 4547 (1987); **37**, 6893 (1988).
 - ⁶ M. Gell, Phys. Rev. B **38**, 7535 (1988).
 - ⁷ T. P. Pearsall, J. Bevk, J. C. Bean, J. M. Bonar, J. P. Mannaerts, and A. Ourmazd, Phys. Rev. B **39**, 3741 (1989).
 - ⁸ F. Cerdeira, M. I. Alonso, D. Niles, M. Garriga, M. Cardona, E. Kasper, and H. Kibbel, Phys. Rev. B **40**, 1361 (1989).
 - ⁹ R. Zachai, K. Eberl, G. Abstreiter, E. Kasper, and H. Kibbel, Phys. Rev. Lett. **64**, 1055 (1990).
 - ¹⁰ U. Schmid, F. Lukeš, N. E. Christensen, M. Alouani, M. Cardona, E. Kasper, H. Kibbel, and H. Presting, Phys. Rev. Lett. **65**, 1933 (1990).
 - ¹¹ J. L. Freeouf, J. C. Tsang, F. K. LeGoues, and S. S. Iyer, Phys. Rev. Lett. **64**, 315 (1990).
 - ¹² U. Schmid, J. Humlíček, F. Lukeš, M. Cardona, H. Presting, H. Kibbel, E. Kasper, K. Eberl, W. Wegscheider, and G. Abstreiter, Phys. Rev. B **45**, 6793 (1992).
 - ¹³ P. A. M. Rodrigues, F. Cerdeira, M. Cardona, E. Kasper, and H. Kibbel, Solid State Commun. **86**, 637 (1993).
 - ¹⁴ L. Viña, S. Logothetidis, and M. Cardona, Phys. Rev. **30**, 1979 (1984).
 - ¹⁵ P. A. M. Rodrigues, F. Cerdeira, and J. C. Bean, Phys. Rev. B **46**, 15 263 (1992).
 - ¹⁶ A. Daunois and D. E. Aspnes, Phys. Rev. B **18**, 1824 (1978).
 - ¹⁷ M. Garriga, M. Cardona, N. E. Christensen, P. Lautenschlager, T. Isu, and K. Ploog, Phys. Rev. B **36**, 3254 (1987).
 - ¹⁸ F. Cerdeira, A. Pinczuk, T. H. Chiu, and W. T. Tsang, Phys. Rev. B **32**, 1390 (1985).
 - ¹⁹ J. C. Tsang, S. S. Iyer, J. A. Calise, and B. A. Ek, Phys. Rev. B **40**, 5886 (1989).
 - ²⁰ R. Hull and J. C. Bean, in *Semiconductors and Semimetals*, edited by T. P. Pearsall (Academic Press, New York, 1991), Vol. 33, p. 1.
 - ²¹ F. Cerdeira, A. Pinczuk, J. C. Bean, B. Blatog, and B. A. Wilson, Appl. Phys. Lett. **45**, 1138 (1984).
 - ²² M. I. Alonso, F. Cerdeira, D. Niles, M. Cardona, E. Kasper, and H. Kibbel, J. Appl. Phys. **66**, 5645 (1989).
 - ²³ D. E. Aspnes, in *Handbook on Semiconductors*, edited by T. S. Moss (North-Holland, New York, 1980), p. 109.
 - ²⁴ J. E. Zucker, A. Pinczuk, D. Chemla, A. Gossard, and W. Wiegmann, Phys. Rev. B **29**, 7065 (1984).
 - ²⁵ D. E. Aspnes, Phys. Rev. B **12**, 2297 (1975).
 - ²⁶ The shift of the E_1 , $E_1 + \Delta_1$ transitions in strained bulk-Ge and bulk- $\text{Ge}_{0.7}\text{Si}_{0.3}$ were calculated using deformation potential theory. See, for example, F. H. Pollak and M. Cardona, Phys. Rev. **172**, 816 (1968).
 - ²⁷ R. L. Headrick, J.-M. Baribeau, D. J. Lockwood, T. E. Jackman, and M. J. Bedzyk, Appl. Phys. Lett. **62**, 687 (1993).
 - ²⁸ M. W. C. Dharma-wardana, G. C. Aers, D. J. Lockwood, and J. M. Baribeau, Phys. Rev. B **41**, 5319 (1990).

²⁹ J. C. Tsang, S. S. Iyer, P. Pukite, and M. Copel, Phys. Rev. B **39**, 13 545 (1989).

³⁰ A. Fasolino, E. Molinari, and J. C. Maan, Phys. Rev. B **39**, 3923 (1989).

³¹ M. A. Renucci, J. B. Renucci, and M. Cardona, in *Proceedings of the Second International Conference on Light Scattering on Solids*, edited by M. Balkanski (Flammarion,

Paris, 1971), p. 326.

³² Room temperature ER and PR spectra have lower intensity and much poorer resolution. The value of the E_1 -like transitions for room temperature can be estimated from the known temperature dependence of the E_1 structure in bulk-Ge and Si (see Ref. 14) by downshifting the values in Table II by ~ 0.12 eV.